RI 8227

Bureau of Mines Report of Investigations/1977

Shock Loss Calculations Across Junctions and Splits

UNITED STATES DEPARTMENT OF THE INTERIOR

Report of Investigations 8227

Shock Loss Calculations Across Junctions and Splits

By John C. Edwards and Henry E. Perlee

UNITED STATES DEPARTMENT OF THE INTERIOR
Cecil D. Andrus, Secretary

BUREAU OF MINES

This publication has been cataloged as follows:

Edwards, John C

Shock loss calculations across junctions and splits / by John C. Edwards and Henry E. Perlee. [Washington] : Bureau of Mines, 1977.

9 p. : diagrams ; 26 cm. (Report of investigations - Bureau of Mines ; 8227)

Bibliography: p. 9.

1. Mine ventilation. 2. Air ducts. 3. Shock (Mechanics). I. Perlee, Henry E., joint author. II. United States. Bureau of Mines. III. Title. IV. Series: United States. Bureau of Mines. Report of investigations - Bureau of Mines ; 8227.

TN23.U7 no. 8227 622.06173

U.S. Dept. of the Int. Library

CONTENTS

ILLUSTRATIONS

SHOCK LOSS CALCULATIONS ACROSS JUNCTIONS AND SPLITS

by

John C. Edwards[1] and Henry E. Perlee[2]

ABSTRACT

A computer code for laminar, steady-state, incompressible, two-dimensional flow developed by Gosman (2)[3] was modified by the Bureau of Mines to calculate shock (minor) loss at the intersections of ventilation ducts. Turbulent flow was simulated using laminar flow equations and an appropriate wall shear stress. Results of the calculation showed good agreement with the experiment.

INTRODUCTION

One of the major problems associated with underground coal mining operations concerns the design of adequate ventilation systems. Because a coal mine may extend for miles in both directions and may have a high-density of passageway intersections, the pressure head losses (shock loss or minor loss) that occur at these intersections become an important ventilation characteristic. The only information presently available in the literature pertaining to such losses has resulted from a few experimental studies (3-4, 7). It is of value, in the interest of designing minimum loss ventilation systems for underground coal mines, to be able to calculate these shock losses from fundamental concepts. With this objective, this investigation was undertaken by the Bureau of Mines. The model makes use of an available laminar flow code development by Gosman, and appropriate wall shear boundary conditions to simulate turbulent mean flow. The results of the calculation show good agreement with measured shock losses.

DESCRIPTIVE EQUATIONS

Figure 1 shows the geometry of the split and junction intersections considered in this study. The computer code used to calculate the shock at the split and junction intersections is a modification of a computer program (2)

---

[1] Physicist.
[2] Supervisory research chemist.
Both authors are with the Pittsburgh Mining and Safety Research Center, Pittsburgh, Pa.
[3] Underlined numbers in parentheses refer to items in the list of references at the end of this report.

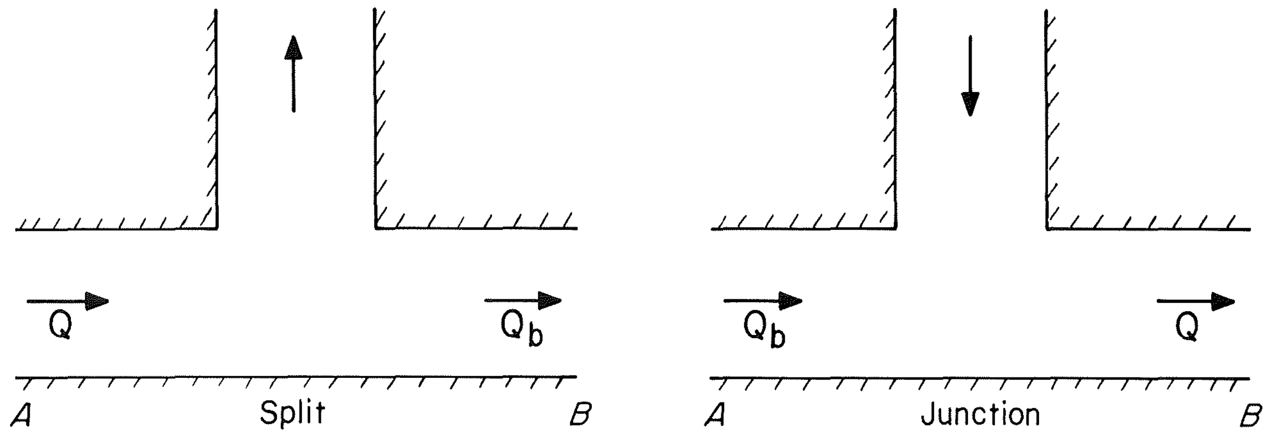

FIGURE 1. - Schematic of the split and junction.

for steady-state flow. The model described is based upon the Navier-Stokes equations for two-dimensional, laminar, steady, viscous incompressible flow. The computer code was modified to include a calculation of the pressure head loss between A and B of the two sections in the straight branch of the 90° junction or split. In this calculation, all passageways have the same cross sectional area even though the code is not limited to this situation. The shock loss, H_x, across an intersection is traditionally assumed to be proportional to the upstream velocity head H_v according to the expression (7),

$$H_x = x\, H_v \,, \tag{1}$$

where H_v is the velocity head at the upstream section, for example A, and equal to $1/2\ V^2$, where V is the flow velocity (an average cross-sectional velocity) and x is the proportionality factor called the shock loss factor. The flow treated here is incompressible. The shock loss H_x does not refer to losses associated with compressible gases. According to pipe flow studies, the shock loss H_x between sections A and B can be written (3)

$$H_x = \frac{P_A - P_B}{\rho} + \frac{1}{2}\,(V_A^2 - V_B^2) - H_f \,, \tag{2}$$

where H_f is the wall drag head loss and $P_A - P_B$ is the average pressure drop between sections A and B. Sections A and B between which the shock loss is calculated are selected sufficiently distant from the intersection that the flow is uniform and the pressure gradient is small. In this calculation, A and B are 6 to 7 diameters from the junction, and the deflected branch is at least 3 diameters in length. For a split, the volumetric flow rate of the entering fluid is designated by Q, and the volumetric flow rate of the fluid that exits through the straight branch is designated by Q_b. For a junction, the volumetric flow rate of the fluid that enters through the straight branch is designated by Q_b, and the volumetric flow rate of the fluid that exits through the straight branch is designated by Q. The calculations for shock loss in this report are limited to the straight branch.

Preliminary studies showed that for a junction with $Q_b/Q = 0.31$ increasing the deflected branch length from 3 to 24 diameters and the downstream branch from 7 to 14 diameters increased the shock loss factor in the straight branch less than 5 pct. Furthermore, decreasing the numerical mesh size by 20 pct in the finite difference computational procedure increased the shock loss factor by 5 pct. Velocities and Reynolds numbers at station B in these calculations ranged from 51 cm sec^{-1} and 8×10^4 to 127 cm sec^{-1} and 2×10^5, respectively.

The pressure drop between stations A and B was calculated using the expression

$$P_B - P_A = \int_A^B \left(\frac{\partial P}{\partial x}\right)_y dx, \tag{3}$$

which was numerically evaluated using values of $\left(\frac{\partial P}{\partial x}\right)_y$ obtained from the numerical solution.

The upstream velocity and the velocity at the branch inlet (for junctions) or outlet (for splits) were constant over the duct cross section and specified by means of the stream function as shown in figure 2.

The stream function is assigned a constant value along the duct walls, and varies linearly across the inlet of the main branch and the inlet (outlet) of the junction (split) as shown in figure 2.

The vorticity along the walls is determined by way of a no-slip boundary condition and a Taylor series expansion of the stream function normal to the wall as described by Gosman except for the corner point P. At P the vorticity is evaluated explicitly. In all calculations the viscosity was 1.8×10^{-4} gm cm^{-1} sec^{-1}.

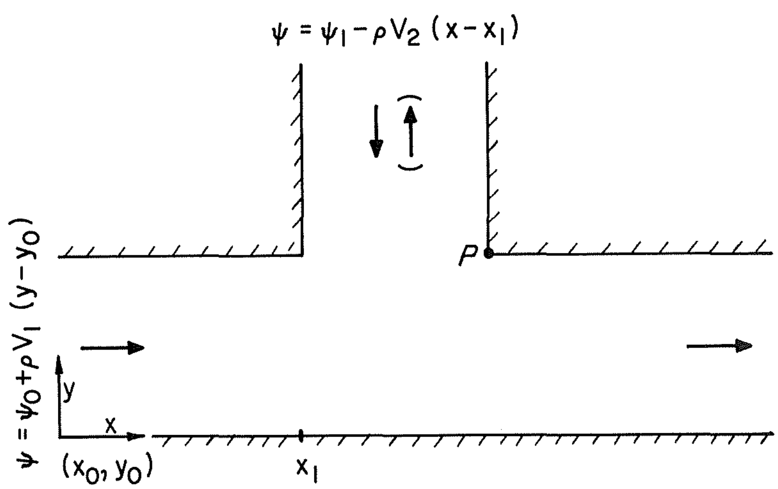

FIGURE 2. - Prescription of stream function at inlet of main branch and inlet or outlet of deflected branch.

A test was run to demonstrate the development of parabolic flow and the minor importance of friction loss in these calculations. A uniform flat velocity profile defined at the inlet of the two-dimensional duct without junctions or splits and with a no-slip boundary condition on the walls developed immediately downstream into slightly asymmetric cross-sectional velocity distribution with slightly increasing values away from the walls. The lack of symmetry in the velocity is probably due to numerical inaccuracies (truncation). Evaluation of the friction loss using equation 2 with $H_x = 0$ for an inflow velocity of 102 cm sec^{-1} gave $H_f = -50$ cm^2 sec^{-2}. Such a friction loss is negligible compared with the split and junction shock losses for comparable velocities. Consequently, H_f was neglected in subsequent calculations.

RESULTS

Laminar Calculation

Because the friction heat loss (H_f) was found to be negligible in this laminar flow model compared with the total head loss for these short branch lengths, the H_f term was neglected in equation 2. Only for very long tunnels would the friction loss become appreciable. Figures 3 and 4 show the calculated stream lines for a junction with $Q_b/Q = 0.5$ and a split with $Q_b/Q = 0.7$. The main difference between these two systems is the presence of the recirculation region that developed for the split, but not for the junction. A finer numerical grid could bring the flow separation point of $\psi = 14$ in figure 3 closer to the corner where it is expected. Hartman (4) in his experiments observed a recirculation region for both the junction and the split. Figure 5 shows the calculated shock loss in the straight branch for the 90° junction and split (for no-slip boundary condition denoted by $\beta = \infty$) as a function of Q_b/Q. Figure 5 also shows values that are estimated from the experimental results reported by Hartman for a rectangular cross section duct. Shock loss factors for a split were calculated for Q_b/Q from 0.655 to 0.885. Attempts to solve the equations for $Q_b/Q < 0.655$ resulted in very large recirculation regions in the 90° duct that always appeared to extend to the exit of the duct making a selection of the exit boundary conditions questionable. For this reason, no calculated values are available for a split with $Q_b/Q < 0.655$. Over the limited range available for comparison, the calculated split shock loss factors agree with those obtained from Hartman's studies.

Figure 3 shows that although both the calculated and measured shock loss factors for a junction exhibit a hyperbolic dependence on Q_b/Q, the quantitative agreement is poor (about 100 pct difference at $Q_b/Q = 0.3$). Because the Reynolds number is large, a turbulent calculation is called for. This was simulated by using laminar equations to solve the turbulent mean velocity and an appropriate wall shear stress.

To test the sensitivity of the calculated shock loss to the choice of the viscosity, the calculation was repeated for $Q_b/Q = 0.31$ using a molecular viscosity reduced by two orders of magnitude. This resulted in an insignificant change in the shock loss factor for both the split and junction.

The assumption that the shock loss factor is a function of only the ratio Q_b/Q was also tested. This was done by making two junction calculations for $Q_b/Q = 0.315$: one with Q_b and Q equal to 40 and 127 cm sec^{-1}, respectively, and the other with 4.0 and 12.7 cm sec^{-1}, respectively. The first calculation resulted in a shock loss factor of 7.3 and the latter 6.4, showing that decreasing the velocities by a factor of 10 while holding the ratio Q_b/Q

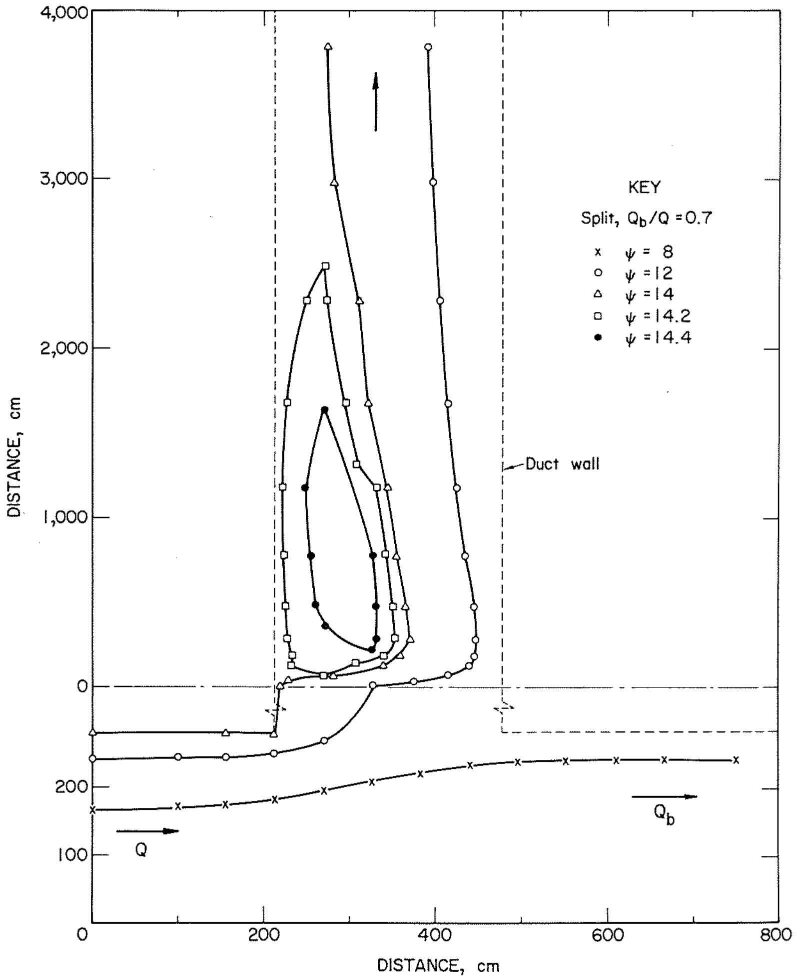

FIGURE 3. - Streamline contours for split ($Q_b/Q=0.7$).

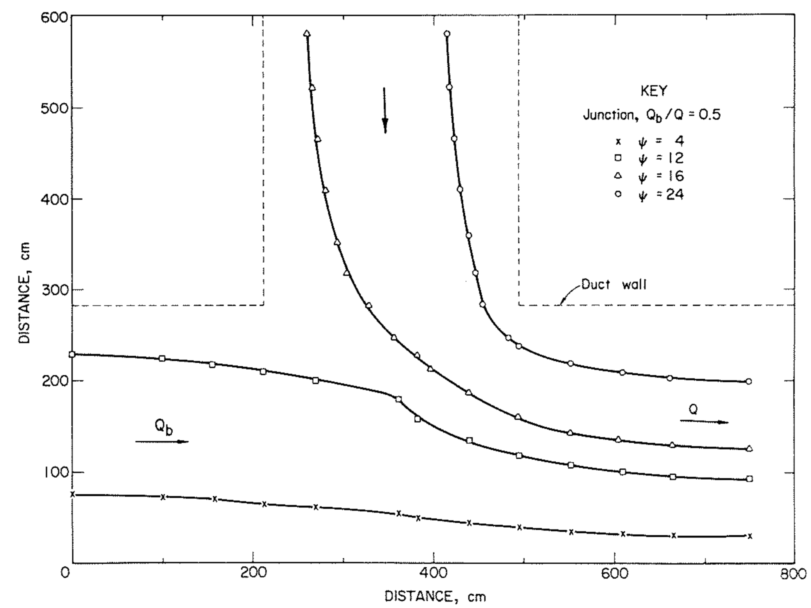

FIGURE 4. - Streamline contours for junction ($Q_b/Q=0.5$).

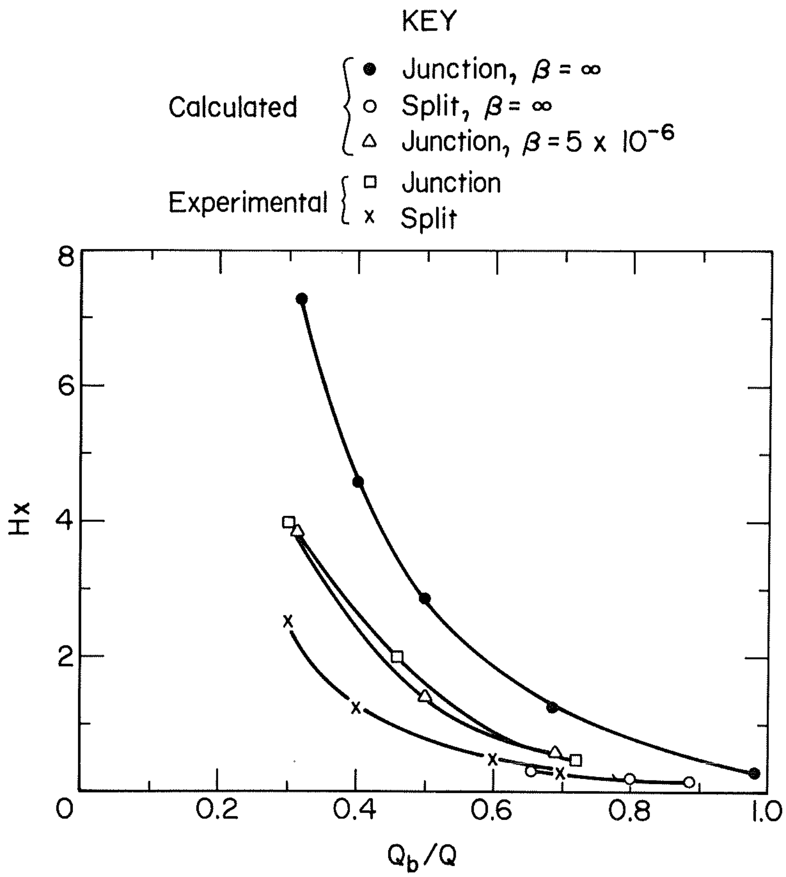

FIGURE 5. - Predicted and experimental shock loss factors.

constant results in a decrease of the shock loss factor of 10 pct.

Other calculations indicate that the shock loss exhibits a strong dependence on the wall boundary condition, that is, slip versus no-slip. The no-slip condition at the wall generates vorticity which is advected and diffused into the main flow where it is subsequently dissipated by viscous forces. The wall vorticity boundary condition for no-slip has been treated here in the manner described by Roache (8) where he derives an expression for the vorticity using a Taylor series expansion of the stream function out from the wall retaining second order terms.

Turbulent Calculation

The significance of no-slip boundary condition can be readily demonstrated by examining the results of a calculation with and without slip at the wall for a junction. For example, for an input velocity in the deflected branch of 87 cm sec^{-1}, and input velocity of 40 cm sec^{-1} in the straight branch, we find a shock loss factor of approximately 7 using no-slip and 0.06 using slip. This illustrates the strong dependence of the calculated shock loss factor upon the wall boundary condition. This could readily account for the 100-pct discrepancy between the calculated and measured values. For the perfect slip condition, no vorticity is generated within the system. This observation suggests that a suitable selection of the expression for the wall shear stress intermediate between slip and no-slip for calculating the wall vorticity might provide more satisfactory agreement with the empirical results. To examine this possibility, a technique reported by Lugt and Ohring (6) was selected in which they used a shear stress (τ) given by the expression

$$\tau = \beta u. \tag{4}$$

The condition of perfect slip is equivalent to $\beta = 0$, and no-slip to $\beta = \infty$. The factor β in equation 2 is related to the coefficient of accommodation (5), which is a measure of the fraction of gas molecules incident on a wall that are absorbed. The introduction of a certain amount of slip through the wall shear stress relationship, equation 4, and the use of laminar flow equations, where the laminar velocity is interpreted as a mean turbulent velocity, is used here to simulate turbulent flow. The vorticity at the wall was modified to include this expression by solving the second order Taylor expansion of the stream function at the wall for the vorticity as discussed by Roache, that is,

$$\Psi_{W+1} = \Psi_W + \left.\frac{\partial\Psi}{\partial y}\right|_W \Delta y + \frac{1}{2}\left.\frac{\partial^2\Psi}{\partial y^2}\right|_W (\Delta y)^2 + 0(\Delta y)^3 , \tag{5}$$

where W is a point on the wall and W + 1 is a point, one mesh point from the wall interior to the gas.

Replacement of the derivatives at the wall in equation 5 by the x-component of the velocity at the wall, namely,

$$U_W = \frac{1}{\rho}\left.\frac{\partial\Psi}{\partial y}\right|_W , \tag{6}$$

and the vorticity at the wall by

$$\omega_W = -\left.\frac{\partial u}{\partial y}\right|_W , \tag{7}$$

results in the expression

$$\Psi_{W+1} = \Psi_W + \rho U_W \Delta y - \frac{1}{2}\rho\omega_W (\Delta y)^2 . \tag{8}$$

Combining equation 4 with the shear stress definition

$$\tau = \mu \frac{\partial u}{\partial y}, \tag{9}$$

and a finite difference expression for the derivative in equation 9 gives the following expression for the tangential velocity at the wall, U_W, with respect to the longitudinal component of the velocity, U_{W+1},

$$U_W = \frac{U_{W+1}}{1 + \frac{\beta}{\mu}\Delta y} . \tag{10}$$

Simultaneous solution of equations 8 and 10 for the wall vorticity yields

$$\omega_W = -\frac{2}{\rho}\frac{1}{(\Delta y)^2}\frac{\Psi_{W+1} - \Psi_W}{\frac{\mu}{\beta}\frac{1}{\Delta y} + 1} . \tag{11}$$

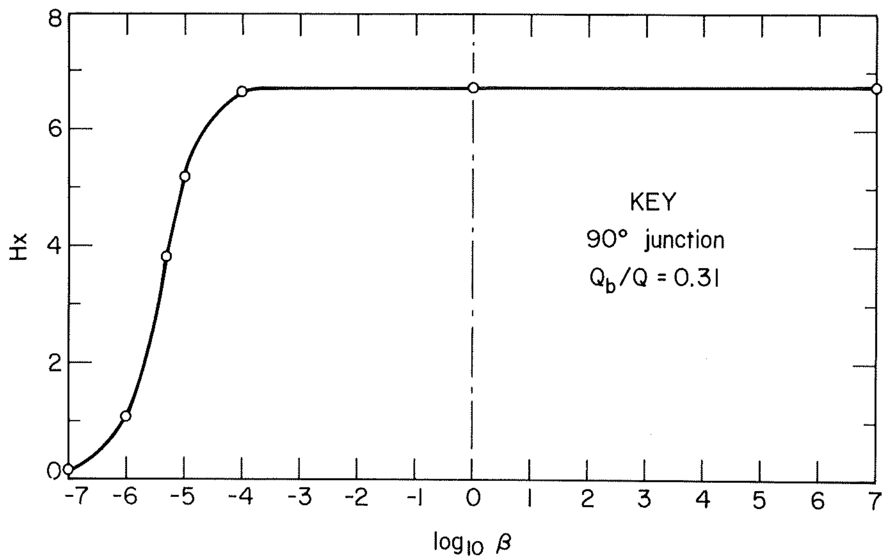

FIGURE 6. - Shock loss factor for a junction for $Q_b/Q=0.31$ with $10^{-7} < \beta < 10^{7}$.

Equation 11 is applied along the wall boundaries, except at the corner point P (see fig. 2), where it is evaluated explicitly in the same manner as all interior points. The finite difference equations for ω and Ψ interior to the duct are discussed in reference 2.

The shock loss factor in a straight branch of a junction with an input velocity of 87 cm sec^{-1} in the straight branch and 40 cm sec^{-1} in the deflected branch ($Q_b/Q = 0.31$) was calculated for values of β ranging from 10^{-7} to 10^{7}. The results of the calculation are shown in figure 6. Figure 6 shows that the transition from slip to no-slip occurs at values of β corresponding to about 10^{-4}. The results in figure 6 also show that, if we choose $\beta = 5 \times 10^{-6}$, then the shock loss factor agrees with the corresponding empirical value (for $Q_b/Q = 0.31$) shown in figure 5. A recalculation of the shock loss factor with $\beta = 5 \times 10^{-6}$ for two additional values of Q_b/Q for the junction gave excellent agreement with the empirical values of the shock loss factors as shown in figure 5. It remains for future investigations to determine if this value of β is unique, that is, if it might also be a function of the geometry of the intersection.

CONCLUSIONS

The computer code cited in reference 1, supplemented by the wall shear boundary condition, $\tau = \beta u$, yields encouraging results, but additional tests are required to assess the utility and range of applicability of the model. Although for the large Reynold's numbers considered in these calculations, $Re \gtrsim 10^4$, a turbulent computation should be made; it appears that through the augmentation of the wall shear stress definition made in equation 4, a suitable predictive capability was achieved with otherwise laminar flow equations. In particular, calculated shock loss in the straight branch at such intersections shows good agreement with corresponding measured values. It has also been shown that shock losses at intersections are, for the most part, functions of the ratio of the inlet and outlet velocities and relatively independent of their magnitudes.

It will require further experimental and numerical studies before a model sufficient for design purpose is developed. Future numerical work should include three-dimensional effects and an exploration of turbulent models.

REFERENCES

1. Eckert, E. R. G., and R. M. Drake, Jr. Heat and Mass Transfer. McGraw-Hill Book Company, Inc., New York, 1959, pp. 154-155.

2. Gosman, A. D., W. M. Pun, A. K. Runchal, D. B. Spalding, and M. Wolfshtein. Heat and Mass Transfer in Recirculating Flows. Academic Press, London and New York, 1969, 338 pp.

3. Hartman, H. L. Mine Ventilation and Air Conditioning. The Ronald Press Company, New York, 1961, pp. 74-77.

4. _____. Pressure Changes at Splits and Junctions in Mine Ventilation Circuits. Trans. AIME, v. 217, 1960, pp. 163-170.

5. Huang, K. Statistical Mechanics. John Wiley & Sons, Inc., New York, 1966, pp. 109-110.

6. Lugt, H. J., and S. Ohring. Laminar Flow Behavior Under Slip-Boundary Conditions. Phys. Fluids, v. 18, No. 1, January 1975, pp. 1-8.

7. McElroy, G. E. Engineering Factors in the Ventilation of Metal Mines. BuMines Bull. 385, 1935, p. 46.

8. Roache, P. J. Computational Fluid Dynamics. Hemosa Publishers, Albuquerque, N. Mex., 1972, p. 141.

☆ U.S. GOVERNMENT PRINTING OFFICE: 1977-703-001/61

INT.-BU.OF MINES,PGH.,PA. 22140